Conformational Transitions in tRNA^{Asp} (Brewer's Yeast). Thermodynamic, Kinetic, and Enzymatic Measurements on Oligonucleotide Fragments and the Intact Molecule†

Stephen M. Coutts,*,‡ Jean Gangloff,§ and Guy Dirheimer§

ABSTRACT: Melting curve measurements have been made on the rT-ψ arm, the CCA and pU halves, and the intact molecule of tRNA^{Asp} (yeast). The major findings may be summarized as follows. (1) The rT-ψ arm melts with a T_m of 79° and has a ΔH for helix formation of -62 ± 4 kcal/mol in 0.03 M sodium ion, in agreement with its cloverleaf model, which contains five G·C base pairs; relaxation kinetic measurements on this arm have yielded activation enthalpies of 3 ± 6 and 64 ± 6 kcal/mol for helix recombination and dissociation, respectively. (2) The pU half-molecule lacks helical structure in both 5 mM magnesium and 500 mM sodium ion, *i.e.* the isolated dihydrouridine helix does not exist under these conditions. (3) In 5 mM magnesium ion, the two halves recombine to form a structure which can be charged by the cognate synthetase; the magnitude of the enthalpy change observed upon melting the mixed halves implies that either the dihydrouridine helix or the tertiary structure or both form as a consequence of helix formation in the anticodon and acceptor stems. (4) Temperature-jump measurements have been utilized in resolving the melting profile of the intact tRNA^{Asp} in 0.5 M sodium ion; evidence is presented which supports the hypothesis that the first step in the thermal denaturation (with a T_m of 51°) is composed of the simultaneous melting of the tertiary structure, dihydrouridine helix, and acceptor stem, implying that the tertiary structure is able to stabilize the dihydrouridine helix far above its T_m. The final two steps in the thermal denaturation of the molecule are the melting of the anticodon (T_m of 61°) and rT-ψ arm ($T_m > 90°$), respectively.

A detailed knowledge of the tertiary structure and conformational dynamics of tRNA is a prerequisite to understanding its role in protein biosynthesis. The techniques of X-ray crystallography are being applied by several research groups to determine the structure of tRNA (Blake *et al.*, 1970; Cramer *et al.*, 1970; Brown *et al.*, 1972), and the results at 4-Å resolution of one of these investigations have been published (Kim *et al.*, 1973). However, tRNA is a flexible molecule, capable of assuming many conformations, and the function of the different conformations in protein biosynthesis may not be clear on the basis of crystallographic data alone. It is the purpose of this paper to examine a number of conformational transitions in tRNA^{Asp} (yeast) in order to define more fully how the molecule behaves in free solution. The thermodynamic and kinetic properties of several specific tRNA species have been studied in detail (Roemer *et al.*, 1970b; Riesner *et al.*, 1970; Cole *et al.*, 1972; Kearns *et al.*, 1971), and some generalizations may be ventured on the basis of the published data. Conditions may be found (usually through variation of the ionic strength) under which a helix–coil transition, which can be called with virtual certainty the melting of the tertiary structure, occurs before the main body of transitions arising from the melting of the secondary structure, *e.g.* that suggested by the cloverleaf model. The order of the subsequent melting of the arms of the cloverleaf is found to depend upon their G·C content and upon rather complex interdependencies known as "coupling" between the various helix–coil transitions. Conversely, conditions may be found where the tertiary structural transition is more stable than some of the secondary structural elements. In this case it acts as a structure stabilizer or determinant, meaning that until the tertiary structure melts it locks some less stable structural elements in helix form which then melt simultaneously with it. The interplay between secondary and tertiary structural elements is thus of intrinsic interest and is quite likely to be an individual characteristic of each tRNA molecule, *e.g.*, dependent upon the sequence.

The starting point of almost all enzymatic, thermodynamic, and kinetic investigations of tRNA is the universally accepted cloverleaf structure (Zachau, 1969). However, when one considers the four to five separate arms of the cloverleaf, plus the existence of a tertiary structure, and possible false structures (Fresco *et al.*, 1966; Adams *et al.*, 1967) one sees that the melting curves and kinetics of intact tRNA molecules may be very complex. There are ways of resolving this complexity by using different physical methods on the intact tRNA. An alternate approach is to investigate fragments of tRNA and to use the data to interpret the more complex information obtained with the intact molecule (Roemer *et al.*, 1969; Riesner *et al.*, 1973); we have used this approach in our present study. Data are presented on the thermal denaturation curves of the following fragments of tRNA^{Asp} (brewer's yeast): the rT-ψ arm,[1]

† From the Gesellschaft fuer Molekularbiologische Forschung, mBH, 3301 Stoeckheim/Braunschweig, West Germany, and the Université Louis Pasteur, Strasbourg, France. *Received January 21, 1974.* This work was supported by grants from The Deutsche Forschungs Gemeinschaft, SFB 75, the Stiftung Volkswagenwerk, the Centre National de la Recherche Scientifique, L.A. NO. 119, and the Commissariat de l'Energie Atomique, Service de Biologie.

‡ Present address: Department of Biochemical Sciences, Princeton University, Princeton, N. J. 08540.

§ Present address: Institut de Biologie Moleculaire et Cellulaire, du CNRS, Strasbourg, France.

[1] Abreviations used are: rT-ψ arm, the fragment formed by residues 46–64 of tRNA^{Asp} (brewer's yeast); pU and CCA half-molecules, two fragments obtained by cutting tRNA^{Asp} in the anticodon loop, and composed of residues 1–34 and 35–75, respectively; A_{260} unit, the amount of RNA which when dissolved in 1.0 ml of buffer and measured with a 1-cm light path has an absorbance of 1.0 at 260 nm.

CCA and pU halves, and a mixture of the two halves. Physical measurements on fragments of defined sequence can also yield information on the parameters involved in helix–coil transition (Coutts, 1971; Riesner and Roemer, 1973). Thus, we have examined the G·C rich rT-ψ arm in detail. The physical chemical study on the recombination of the two halves is complemented by the measurement of their biological activity with the cognate synthetase, and confirms earlier work with combined fragments of specific tRNA molecules (Wintermeyer *et al.*, 1969; Schmidt *et al.*, 1970). Finally, we have utilized the data obtained with the fragments to complement the physical measurements on the intact molecule, and have proposed a mechanism for the thermal denaturation of tRNA^{Asp} (brewer's yeast).

Materials and Methods

Purification of tRNA^{Asp} and Its Fragments. The method of Keith *et al.* (1971) was used for the preparation of pure tRNA^{Asp} from brewer's yeast. The isolation of the component rT-ψ arm and the pU and CCA half-molecules has been previously published (Gangloff *et al.*, 1972a,b). The sequence analysis of the 3′-terminal half shows that 33% of the molecules did not have the complete CCA terminus.

The aspartyl-tRNA synthetase used in the aminoacylation of the reassociated half-molecules was obtained by a previously described method (Gangloff and Dirheimer, 1973a).

Aminoacylation of the reassociated halves was carried out in 1.0 ml of a reaction mixture containing 0.5 A_{260} unit[1] of each half of the tRNA^{Asp} (which had been heated previously for 5 min at 20° in 0.01 M sodium cacodylate, 0.15 M KCl, 5 mM $MgCl_2$, and 0.5 mM EDTA (pH 7)), 100 μmol of Tris-HCl (pH 7.0), 30 μmol of KCl, 10 μmol of ATP-Na_4, 10 μmol of $MgCl_2$, 100 μg of bovine serum albumin, 2 μmol of reduced glutathione, 0.1 μmol of L-[^{14}C]aspartic acid (50 μCi/μmol), and 5 μg of aspartyl-tRNA synthetase. The aminoacylation was followed as a function of time by taking aliquots of 80 μl from the reaction mixture at given time intervals and pipetting them onto Whatmann No. 3MM paper disks, which were treated according to Mans and Novelli (1961).

Nucleotide Sample Preparation. Oligonucleotide and tRNA samples were stored as precipitates in alcohol at −18° until used. They were phenolized, chromatographed over Sephadex G-25, and concentrated as described by Coutts (1971).

Melting curve measurements were carried out by a modified differential absorption technique (Roemer *et al.*, 1970a), in which the absorbance difference between two independently thermostated cuvets, whose temperature difference is from 2 to 4°, is measured, yielding $\Delta A/\Delta T$. The maximum of the transition peaks (T_m's) observed with this method is equivalent to the point of inflection on the usual integral melting curve. By measuring the absorbance change, ΔA, at two or more wavelengths for each temperature interval, ΔT, one may calculate difference spectrum ratios $\Delta A\lambda_1/\Delta A\lambda_2$. These difference spectrum ratios are very sensitive to the base composition of the helical region undergoing transition (Coutts, 1971) and are thus a diagnostic aid in identifying the secondary structures which are melting. In addition, as a necessary consequence of the "all or none" model for oligonucleotide melting, the difference spectrum ratios must remain constant in order for the peak in the melting curve to be homogeneous, *i.e.* composed of just one transition (Riesner and Roemer, 1973). If the difference spectrum ratios are *not* constant in a peak, it contains two or more transitions.

Samples were heated at 70° for 2 min before each melting curve measurement. Possible degradation occurring during the measurement of the melting curve was checked by cooling the samples back to the temperature of the initial absorbance reading (normally 20°) and comparing the total absorbance with that of the starting solution. It was found experimentally that initial and final absorbancies agreed to within 1%, except when magnesium was present and the samples were measured for long periods above 80°, in which cases differences as high as 3–4% were observed. Such measurements were always repeated. Melting curves measured in the presence of EDTA were corrected for the hyperchromicity of EDTA itself.

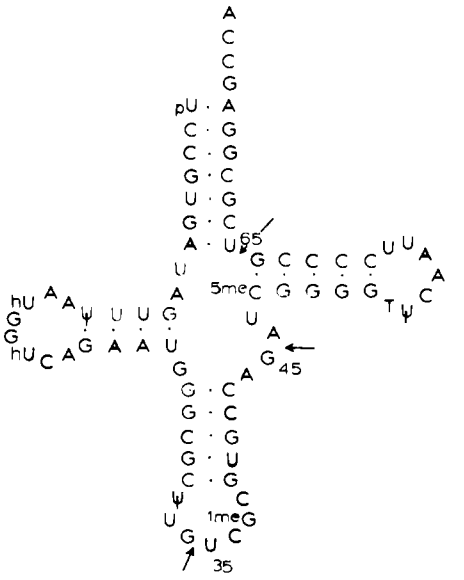

FIGURE 1: The cloverleaf model of tRNA^{Asp} (yeast) according to Gangloff *et al.* (1971). Fragments were isolated from T_1 digests as described in the text. The isolated rT-ψ arm contained residues 46–64. The cleavage to split the molecule into the CCA and pU half-molecules took place between the U and G at positions 35 and 34 of the anticodon loop.

Results

The sequence of tRNA^{Asp} (brewer's yeast) is pictured in Figure 1. The bonds which were cleaved enzymatically to provide the rT-ψ arm and CCA and pU halves are indicated by arrows.

rT-ψ Arm. A differential melting curve of the rT-ψ arm, measured in a buffer containing a low amount of salt, showed two well-resolved transitions, instead of the single transition expected. As Figure 2a demonstrates, two peaks of approximately equal hyperchromicity which have T_m values of 32 and 78.5° are obtained. This result was repeated several times with different preparations and at different ionic strengths. The peak with a T_m of 32°, which we shall call A, has virtually the same difference spectrum ratios ($\Delta A_{260\ nm}/\Delta A_{280\ nm}$) as the peak with a T_m of 78.5° (B). The fact that these ratios are constant throughout each peak and have values of about 0.6 indicates that single "all or none" transitions compose each peak, and that both of these transitions involve the melting of helices containing G·C base pairs only (*cf.* Coutts, 1971; Cox, 1970).

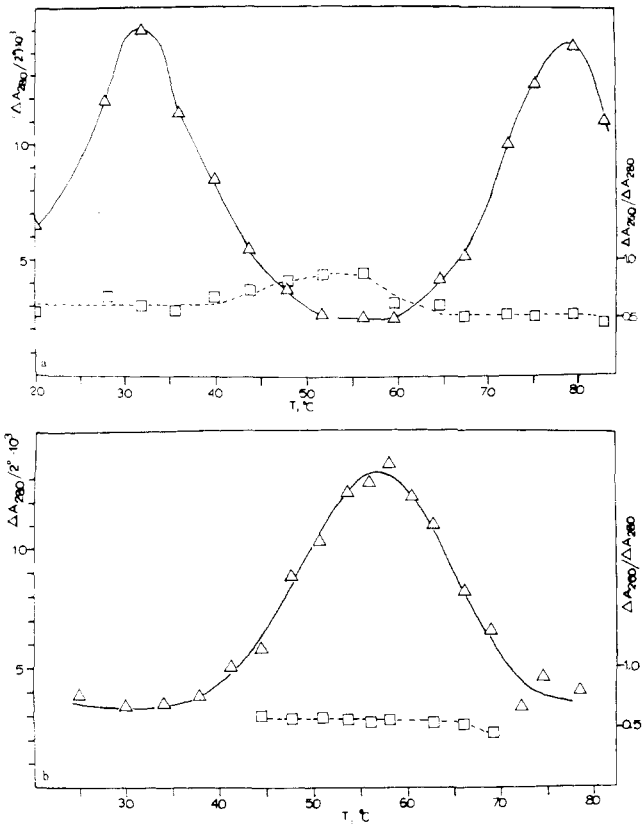

FIGURE 2: (a) The differential melting curve of the rT-ψ arm of $tRNA^{Asp}$ in 0.01 M sodium cacodylate, 0.02 M sodium chloride, and 1 mM EDTA (pH 6.8). The $A_{260\ nm}$ of the solution at 20° was 2.0, which was equivalent to $A_{280\ nm}$ of 0.93; difference spectrum ratios: (□- -□) $\Delta A_{260\ nm}/\Delta A_{280\ nm}$; (Δ-Δ) $\Delta A_{280\ nm}/2°$. (b) The differential melting curve of transition A in 0.01 M sodium cacodylate, 1.0 M sodium chloride, and 1 mM EDTA (pH 6.8). The absorbance of the solution at 280 nm and 20° was 1.24: (Δ-Δ) $\Delta A_{280\ nm}/2°$; (□- -□) difference spectrum ratios $\Delta A_{260\ nm}/\Delta A_{280\ nm}$.

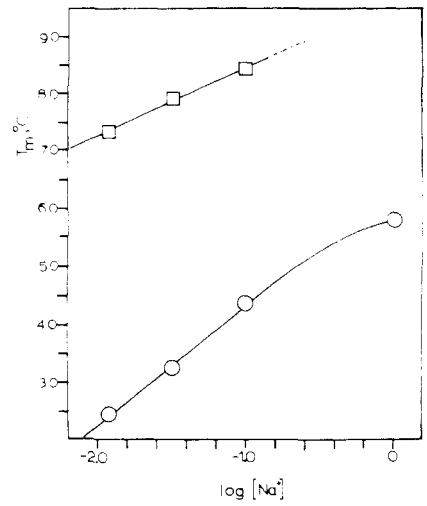

FIGURE 3: The dependence of the transition midpoints of transitions A and B of the rT-ψ arm upon the ionic strength. Sodium chloride was added to a solution of 0.01 M sodium cacodylate–1 mM EDTA (pH 6.8) to achieve the desired ionic strengths. The absorbance at 260 nm and 20° of the solution used for T_m^A was 1.7: (O-O) T_m points for transition A; (□- -□) T_m points for transition B.

The T_m and temperature-jump kinetics of A showed a dependence upon concentration; those of transition B did not. In addition, as shown in Figure 3, the dependencies upon ionic strength of the two transitions differ considerably. Effect A has $dT_m/d \log [Na^+]$ equal to 23 ± 3°, while effect B has a value of 12 ± 3°; the latter value is normal for a hairpin helix the size of the rT-ψ arm (Scheffler *et al.*, 1968). Although the melting curves for the rT-ψ arm exhibit two peaks, the disc electrophoretic patterns in 7 M urea for the same sample contained just one band. Similarly, an attempt to separate the components responsible for the two effects by chromatography over DEAE-cellulose in 7 M urea at pH 7.5 yielded only one chromatographic peak which, after the removal of urea and salt by successive chromatographic steps over DEAE-cellulose and Sephadex G-25 (fine), gave a melting curve identical with the previous one.

Thus, although the melting curve shows heterogeneity, several analytical methods indicate that the rT-ψ arm preparation is homogeneous. Apparently a double-stranded helix containing five G·C pairs remains helical in 7 M urea when there is enough salt in the gradient to raise the T_m above room temperature. Another example of this behavior is the isolated double-stranded acceptor stem of $tRNA^{Tyr}$ (*Escherichia coli*), which contains five contiguous G·C base pairs, and which also remains undissociated in 7 M urea when chromatographed over DEAE-cellulose (D. Riesner, personal communication).

The independence of the temperature-jump kinetics from concentration, the difference spectrum ratios of 0.55 and the moderate dependence of T_m upon sodium ion concentration (12°) are all consistent with the assignment of transition B to the helix–coil transition of the rT-ψ arm as written in the cloverleaf structure (Figure 1). In addition, the high T_m (80°) in 30 mM sodium ion is similar to that of another oligonucleotide, the extra arm of $tRNA^{Ser}$ (yeast) (Coutts, 1971), which contains three–four G·C base pairs and is typical of the stability displayed by hairpin helices (Scheffler *et al.*, 1968; Uhlenbeck *et al.*, 1973). The data of Gralla and Crothers (1973) can be used to calculate the stability of the helix in 1 M sodium ion, yielding the value of 100° for T_m. Extrapolation of the ionic strength dependence curve for the T_m values of transition B (Figure 3) to 1 M sodium ion gives 97 ± 2°, which is in excellent agreement with the calculated value. However, Gralla and Crothers' enthalpy value for G·C base pairing (12.7 kcal/mol) disagrees substantially with the value obtained from the present study (*vide infra*), indicating that their data may not represent the best fit of the entropic and enthalpic parameters.

Two alternatives present themselves for the identity of transition A: either the arm dimerizes, or the hairpin loop has been cut in roughly 50% of the molecules. Two facts argue against the existence of dimers. If dimers were responsible for effect A, the only additional base pairs besides the ten G·C pairs of the cloverleaf which could be formed would be A·U. This is not the case, as is seen from the difference spectrum ratios, which would change from 0.55 to 0.9 with the addition of just one A·U base pair to five G·C (Coutts, 1971). In addition, the expected enthalpy (and hyperchromic) change upon the melting of dimers containing no additional base pairs would be close to zero, since the hairpin products would have the same number of base pairs. The observed enthalpy change of −78 kcal/mol negates this alternative. Thus, on the basis of the physical evidence above, the rT-ψ arm is susceptible to cleavage sometime in the course of its isolation, perhaps being cut at the G residue at position 52 which has its 3′ end adjoining the nonhelical loop. A working hypothesis in the analysis of the thermodynamic and kinetic data for the rT-ψ arm was that transition A represented the helix–coil transition of the arm with a cut somewhere in the loop. The second transition (B) was assumed

to represent the intact arm. Thus, the following equilibria were considered

$$C_1 + C_2 \underset{k_D'}{\overset{k_R'}{\rightleftharpoons}} H' \text{ (transition A)} \quad (1)$$

$$C \underset{k_D}{\overset{k_R}{\rightleftharpoons}} H \text{ (transition B)} \quad (2)$$

where H′ is the nicked helix, H the intact helix, and C_1, C_2, and C are the randomly coiled products of the helix–coil transition. The rate constants for helix dissociation and recombination are k_D and k_R, respectively. In order to make the kinetics of the first transition fast enough for convenient measurement with the temperature-jump apparatus, they were measured using a buffer containing 1 M sodium chloride. The melting curve for effect A in the 1 M sodium ion is shown in Figure 2b. At this ionic strength, transition A has a T_m of approximately 58°, depending upon the nucleotide concentration. The kinetics of the second transition were measured in 0.02 M sodium chloride–10 mM sodium cacodylate (pH 6.8); these low salt conditions were necessary to slow down the reaction so that it was still measurable, and yet still provide enough salt so that the heating rise time of the temperature jump was appreciably faster than the relaxation time for the oligonucleotide. The relaxation kinetic equations for the equilibria in eq 1 and 2 are given in eq 3 and 4, respectively, where τ is the relaxation time.

$$1/\tau = k_R([C_1] + [C_2]) + k_D \quad \text{(bimolecular)} \quad (3)$$

$$1/\tau = k_R + k_D \quad \text{(monomolecular)} \quad (4)$$

In the bimolecular case the concentrations of the reactants must be known in order to evaluate the rate constants. Although the concentration of the nicked arm was not known, the equilibrium and rate constants for transition A could be analyzed as a product of total nucleotide concentration to yield reaction and activation enthalpies, according to eq 5 and 6 and

$$K[H]_0 = (1 - \theta)/\theta^2 = (k_R/k_D)[H]_0 \quad (5)$$

$$k_R[H]_0 = \frac{1}{\tau}\left(\frac{1-\theta}{\theta^2}\right)\frac{1}{\sqrt{4\left(\frac{1-\theta}{\theta^2}\right)+1}} \quad (6)$$

standard van't Hoff and Arrhenius treatments. $[H]_0$ is the total helix concentration (or total concentration of one half), θ is the extent of reaction, which is obtained by integration of the melting curve, and τ is the relaxation time. Equations 5 and 6 are derived in the Appendix to this paper. van't Hoff and Arrhenius plots for transitions A and B are displayed in Figure 4, and the thermodynamic and kinetic parameters obtained from these plots are given in Table I.

Isolated pU and CCA Halves. Two conditions were chosen for the examination of the differential melting curves of the separated and combined pU and CCA halves of tRNA^{Asp}. One set of conditions consisted of a buffer containing 10 mM sodium cacodylate and 5 mM magnesium chloride (pH 6.8), which approximated the conditions under which the enzymatic charging of the half-molecules was measured. Thermodynamic and kinetic data obtained in the presence of magnesium, however, can be complicated by the binding equilibria of magnesium with the oligonucleotides. Thus, the second set of conditions employed a magnesium-free buffer containing 10 mM sodium cacodylate, 1 mM EDTA, and 0.5 M sodium chloride (pH 6.8).

The melting curves of the isolated half-molecules were qualitatively similar under both sets of conditions (Figure 5). The CCA half-molecule shows no transition other than the melting

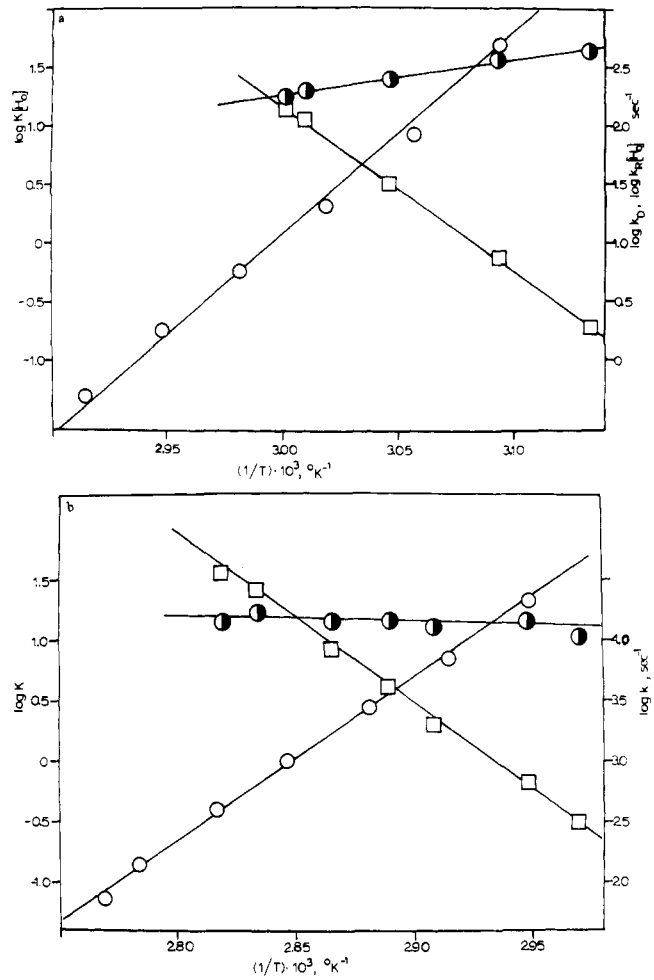

FIGURE 4: (a) van't Hoff and Arrhenius plots for transition A of the rT-ψ arm. The buffer was 0.01 M sodium cacodylate, 1.0 M sodium chloride, and 1 mM EDTA (pH 6.8): (○–○) logarithm of the product of the equilibrium constant and the total nucleotide concentration, log $(K[H]_0)$; (◑–◑) logarithm of the product of the rate constant for recombination and the total nucleotide concentration, log $(k_R[H]_0)$; (□–□) logarithm of the rate constant for dissociation, log k_D. (b) van't Hoff and Arrhenius plots for transition B in 0.01 M sodium cacodylate, 0.02 M sodium chloride, and 1 mM EDTA (pH 6.8): (○–○) logarithm of the equilibrium constant, log K; (◑–◑) logarithm of the rate constant for recombination, log k_R; (□–□) logarithm of the rate constant for dissociation, log k_D.

of the rT-ψ arm at high temperatures. If the rT-ψ helix in the CCA half behaves the same as in the isolated rT-ψ arm, it should have a T_m of 93 ± 2° in 0.51 M sodium ion (Figure 3). Although the melting curve for the CCA half-molecule could not be measured beyond 93° in Figure 5b, the observed hyperchromicity, difference spectrum ratios, and peak position are consistent with the rT-ψ helix having identical melting characteristics in both the isolated arm and the half-molecule. In contrast, the hyperchromic change in the pU half was so broad and apparently noncooperative that temperature-jump experiments were carried out on the samples in 0.5 M sodium ion to see whether or not a slow relaxation time, indicative of a helix–coil transition, could be found. The only relaxation effect which could be found over the entire temperature range (20–60°) is normally associated with fast changes in the stacking equilibria of bases in single strands (Riesner and Roemer, 1973).

Mixed Halves. Figure 6 compares the melting behavior of the intact tRNA^{Asp} with mixtures of equal $A_{260\,nm}$ (20°) amounts of the half-molecules. The recombination of the two halves gives rise to a new peak in the melting curve which has

TABLE 1: Thermodynamic and Kinetic Parameters for Helix–Coil Transitions in Fragments and Intact Molecules of $tRNA^{Asp}$ (Brewer's Yeast).[a]

Transition	ΔH (kcal/mol)	ΔS (cal deg^{-1} mol^{-1})	ΔE_R (kcal/mol)	ΔE_D (kcal/mol)	T_M (°C)	$[Na^+]$ (M)
A (rT-ψ arm)	−78 ± 6		−18 ± 6	60 ± 6	58 ± 1	1.01
B (rT-ψ arm)	−62 ± 4	−44 ± 5	3 ± 6	64 ± 6	79.5 ± 1	0.032
I (intact $tRNA^{Asp}$)	−101 ± 5	−78 ± 5	−53 ± 10	48 ± 10	51.4 ± 1	0.51
II (intact $tRNA^{Asp}$)	−71 ± 20	−54 ± 10	−11 ± 10	60 ± 10	61.0 ± 2	0.51
Recombination of CCA and pU halves	−141 ± 10				62.9 ± 1	0.01[b]

[a] Measurements were made at pH 6.8 in 0.01 M sodium cacodylate buffer with 1 mM EDTA and varying amounts of sodium chloride. [b] Contained 5 mM magnesium ion and no EDTA.

more hyperchromicity than the curves of the isolated half-molecules in Figure 5. This constitutes a physical proof that new helical structure(s) arise from the recombination of the two halves. That these helical structures are similar to those found in the native tRNA can be seen in the enzymatic charging experiments with the mixed halves (*vide infra*). It is noteworthy that in contrast to the isolated half-molecules, the recombined half-molecules are much more stable in the presence of 5 mM magnesium ion than in 500 mM sodium ion, with a difference in T_m values of the recombination peaks of about 20°.

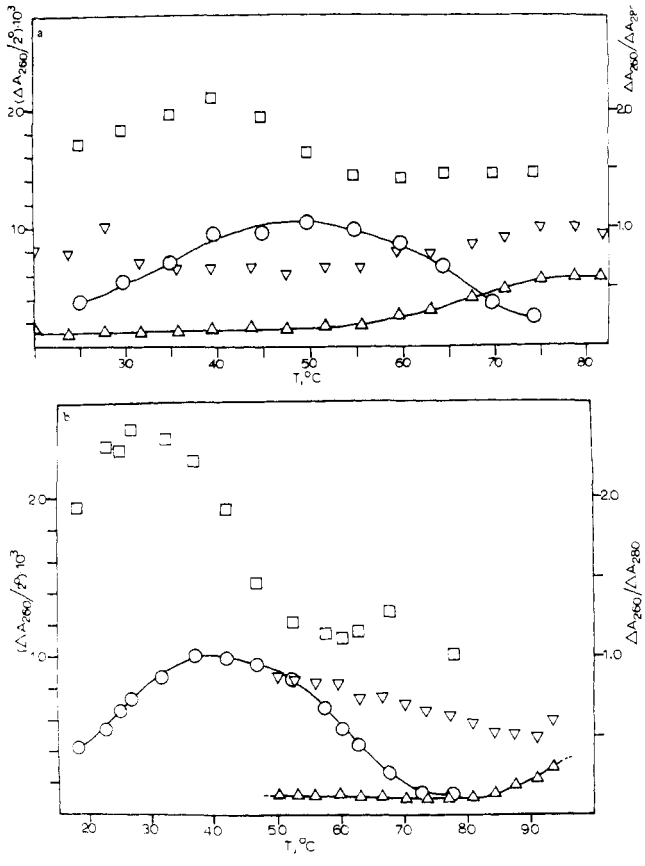

FIGURE 5: (a)Differential melting curves for the pU and CCA halves of $tRNA^{Asp}$, in 0.01 M sodium cacodylate–5 mM magnesium chloride (pH 6.8): (Δ–Δ) $\Delta A_{260\ nm}/2°$, CCA half; (O–O) pU half; (▽–▽) difference spectrum ratios $\Delta A_{260\ nm}/\Delta A_{280\ nm}$ for CCA half; (□–□) difference spectrum ratios for pU half. The absorbance of both solutions at 260 nm and 20° was 1.0. (b) Differential melting curves for the pU and CCA halves of $tRNA^{Asp}$ in 0.01 M sodium cacodylate, 0.5 M sodium chloride, and 1 mM EDTA (pH 6.8). Symbols are the same as in Figure 5a.

Figure 6a also demonstrates that the difference spectrum ratios of the recombination peak measured in 5 mM magnesium ion are constant, having a value of *ca.* 1.8. We conclude that in the presence of magnesium ion, but *not* in the presence of sodium ion, the recombination may proceed in an "all or none" manner, and that eq 1 may be used as a model for the reaction. A van't Hoff plot according to eq 5 of the data in Figure 6a yields a ΔH for helix formation of −141 ± 10 kcal/mol. This is a lower limit of the ΔH involved, since if the "all or none" assumption is not completely fulfilled, the total ΔH value would be even higher.

Aminoacylation of the Reassociated Halves. Figure 7 shows the kinetics of aspartic acid attachment to the two reassociated halves of $tRNA^{Asp}$. It can be seen that the aminoacylation reaction reaches a plateau after about 30 min. Taking into account the fact that only 66% of 3′-terminal halves have an intact CCA end, this plateau corresponds to 61% charging as compared to intact $tRNA^{Asp}$. By increasing the concentration of aspartic acid it is possible to obtain a total charging of all reassociated halves having their 3′-terminal ends intact (Gangloff and Dirheimer, 1973b.)

Melting Behavior of Intact $tRNA^{Asp}$. The differential melting curve of $tRNA^{Asp}$ in 0.5 M sodium chloride is presented in Figure 6b and is characterized by a large peak with a T_m of 53° followed by a long sloping shoulder on the high temperature side. As evidenced by the continually changing difference spectrum ratios (shown in Figure 9), several transitions are embraced by the apparently heterogeneous melting curve. The amplitude of the signal from a temperature-jump experiment is equivalent to the change in absorbance per small temperature interval measured in a differential melting curve. Therefore, a resolution of this mixture of transitions was attempted with the use of relaxation kinetics, since a dynamic (*e.g.*, kinetic) measurement may permit the resolution of the individual transitions according to the time interval in which they take place (Riesner *et al.*, 1970; Cole and Crothers, 1972).

If one assumes the simple two-state "all or none" model of eq 2 for the reaction mechanism of the melting of the structural elements of a tRNA molecule, and that there is no coupling between the transitions, then the differential melting curve associated with a *single* kinetic transition may be calculated according to eq 7, where $A_\tau^*(T)$ is the amplitude of the relaxation effect τ, $A_{total}^*(T)$ is the total relaxation amplitude, $\Delta A(T)/\Delta T$ is the value of the equilibrium differential melting curve, and $A_\tau(T)/\Delta T$ is the value of the differential melting curve associated with the relaxation effect τ, all values being at temperature T, the final temperature of the temperature jump.

$$\Delta A_\tau(T)/\Delta T = (\Delta A(T)/\Delta T)(A_\tau^*(T)/A_{total}^*(T)) \quad (7)$$

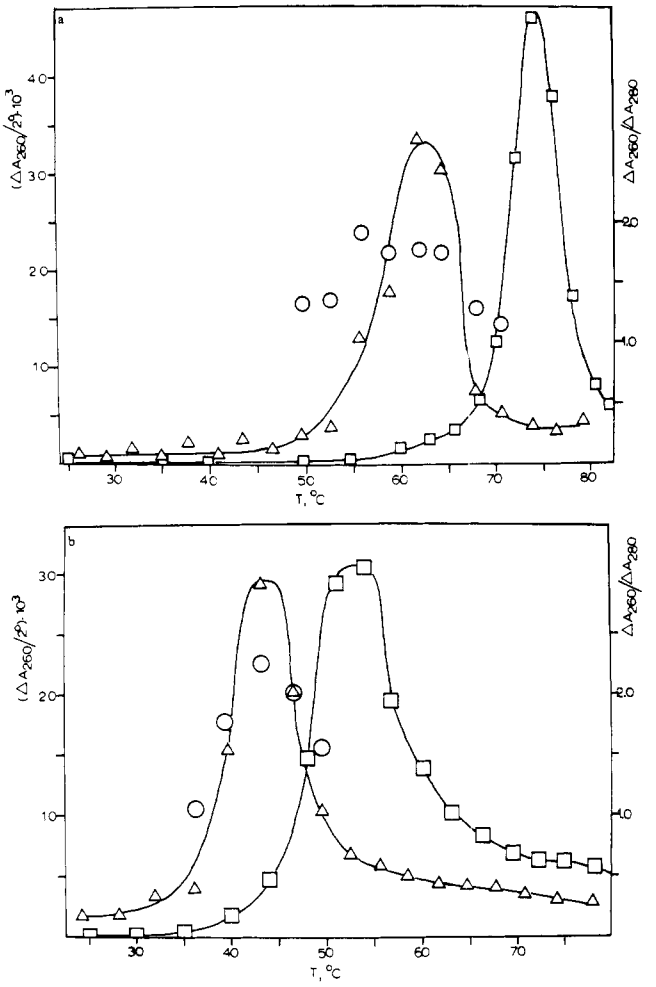

FIGURE 6: (a) Differential melting curves of a mixture of the CCAand pU halves and of the intact tRNA^{Asp}, in 0.01 M sodium cacodylate–5 mM magnesium chloride (pH 6.8): (Δ–Δ) $\Delta A_{260\ nm}/2°$ of a mixture of 0.5 $A_{260\ nm}(20°)$ units each of the pU and CCA halves; (O–O) difference spectrum ratios $\Delta A_{260\ nm}/A_{280\ nm}$ for the recombination peak; (□–□) $\Delta A_{260\ nm}/2°$ of tRNA^{Asp}. The absorbance of the tRNA^{Asp} solution at 20° and 260 nm was 1.0. (b) Differential melting curves of a mixture of the CCA and pU halves, and of the intact tRNA^{Asp}, in 0.01 M sodium cacodylate, 0.5 M sodium chloride, and 1 mM EDTA (pH 6.8): (Δ–Δ) $\Delta A_{260\ nm}/2°$ of a mixture of 0.5 $A_{260\ nm}(20°)$ units each of the CCA and pU halves; (O–O) difference spectrum ratios $\Delta A_{260\ nm}/\Delta A_{280\ nm}$ for the recombination peak; (□–□) $\Delta A_{260\ nm}/2°$ of tRNA^{Asp}. The absorbance of the tRNA^{Asp} solution at 260 nm and 20° was 1.0.

The temperature-dependent equilibrium constants associated with the transitions resolved by relaxation measurements were evaluated from plots of $\Delta A_\tau(T)/\Delta T$ *vs.* T according to Riesner *et al.* (1970), as were the calculations of the transitions' thermodynamic and activation parameters.

Initial kinetic experiments with tRNA^{Asp} in 0.5 M sodium chloride indicated that around 55° three distinct relaxation effects could be seen, which we shall call I, II, and III, and which correspond to relaxation times of 200 msec, 200 μsec, and 5 μsec, respectively. Effect III was equivalent to the heating rise time of the instrument and its origin was therefore ascribed to the perturbation of the single-strand stacking equilibrium. Thus, only effects I and II arise from helix–coil transitions. The corrected amplitudes $\Delta A_\tau/\Delta T$ at 260 nm for effects I, II, and III are plotted in Figure 8, together with the difference spectrum ratios. The curves in Figure 8 are compared to the melting curve of the intact tRNA^{Asp} in Figure 9. The total area under the differential melting curve up to 70° corresponds

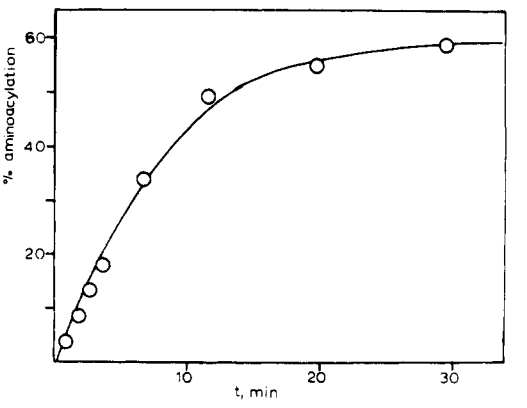

FIGURE 7: The per cent aminoacylation of the recombined half-molecules of tRNA^{Asp} as a function of incubation time with enzyme. Equal A_{260} amounts of isolated CCA and pU halves were mixed and annealed as described in the text, before being treated with purified aspartyl-tRNA synthetase.

to the sum of the amplitudes arising from the three kinetic effects. The points in these plots represent an average calculated with data taken from three to four temperature jumps at a given temperature.

The difference spectrum ratios remain constant throughout the transition in effect I, where $\Delta A_\tau{}^{I}(260\ nm)/\Delta A_\tau{}^{I}(280\ nm)$ has a value of *ca.* 2.7, and throughout effect II, where the value

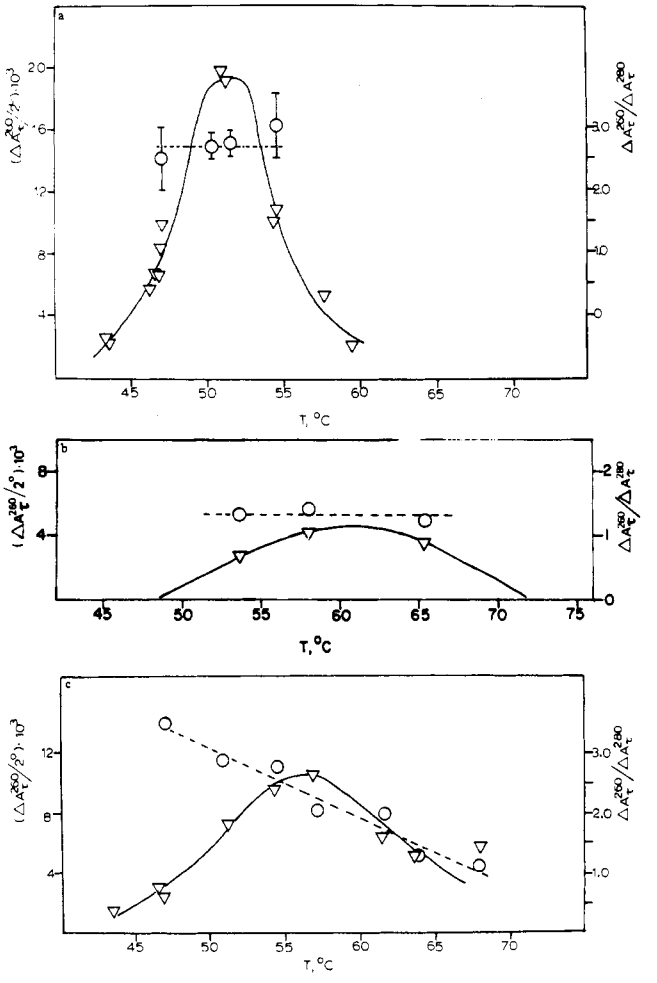

FIGURE 8: (a–c) Corrected relaxation amplitudes for effects I, II, and III, respectively, of tRNA^{Asp} in 0.01 M sodium cacodylate, 0.5 M sodium chloride, and 1 mM EDTA (pH 6.8): (▽–▽) $\Delta A_\tau{}^{260\ nm}/2°$; (O–O) difference spectrum ratios $\Delta A_\tau{}^{260\ nm}/\Delta A_\tau{}^{280\ nm}$. The values are normalized to an absorbance at 260 nm and 20° of 1.0 for tRNA^{Asp}.

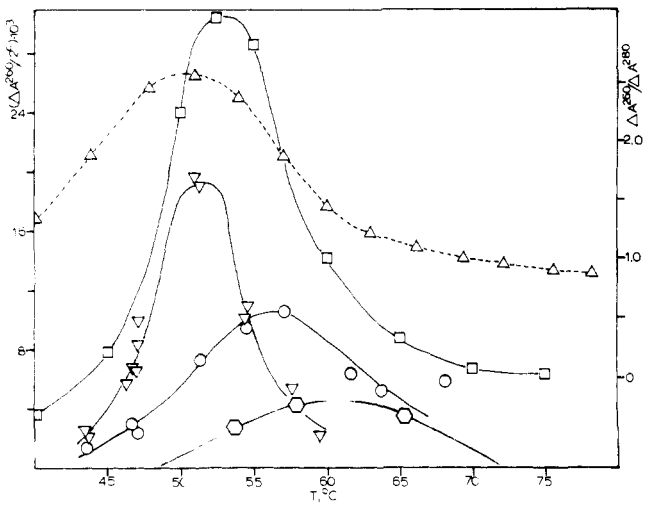

FIGURE 9: A comparison of the relaxation amplitudes for effects I, II, and III with the differential melting curve of $tRNA^{Asp}$, in 0.01 M sodium cacodylate, 0.5 M sodium chloride, and 1 mM EDTA (pH 6.8): (□-□) $\Delta A_{260\ nm}/2°$ for $tRNA^{Asp}$; (▽-▽) $\Delta A_{\tau}^{260\ nm}/2°$ for effect I; (○-○) effect II; (○-○) effect III; (△-△) difference spectrum ratios $\Delta A_{260\ nm}/\Delta A_{280\ nm}$ for $tRNA^{Asp}$.

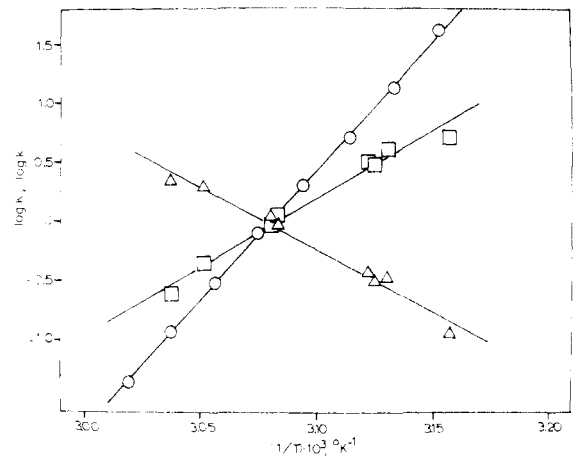

FIGURE 10: van't Hoff and Arrhenius plots for effect I of intact $tRNA^{Asp}$ in 0.01 M sodium cacodylate, 0.5 M sodium chloride, and 1 mM EDTA (pH 6.8): (○-○) logarithm of the equilibrium constant, K; (□-□) logarithm of the rate constant for recombination, k_R; (△-△) logarithm of the rate constant for dissociation, k_D.

is *ca.* 1.3. Integration of the melting curve for effect I in Figure 8a leads to values of K which are plotted as a function of temperature in Figure 10. Included in Figure 10 are values for k_R and k_D. The thermodynamic and activation parameters gained from Figure 10 are listed in Table I.

Because of its cooperativity and large difference spectrum ratios, effect I coincides with the major peak of the intact $tRNA^{Asp}$ melting curve at 260 nm. Melting curves of the intact molecule were measured at different ionic strengths to determine the dependence upon ionic strength of effect I, which was found to be $dT_m^I/d \log [Na^+] = 17 \pm 3°$.

Discussion

Measurements were performed on the fragments of $tRNA^{Asp}$ with a twofold purpose: to obtain thermodynamic and kinetic data on the isolated rT-ψ and dihydrouridine arms to aid in the interpretation of the melting of the intact molecule, and to present physical evidence for the reconstitution of the two half-molecules.

Physical Parameters of the Isolated rT-ψ Arm. The rT-ψ arm of $tRNA^{Asp}$ contains, on the basis of its cloverleaf structure (Figure 1), five G·C base pairs, with one of the cytosines methylated on the number five carbon. Several pieces of evidence have been presented which indicate that the second transition, B, in the melting curve of the oligonucleotide represents the helix to coil transition of the base pairs suggested in the cloverleaf model.

The enthalpy change for helix-coil transition B can be reasonably interpreted as arising from four nearest neighbor interactions; the formation of the first base pair, or the nucleation of the helix, involves hydrogen bond formation only and no stacking, and consequently should have an enthalpy change close to zero. Thus, the change in enthalpy for the addition of a G·C base pair to an existing helix in the rT-ψ arm of $tRNA^{Asp}$ would be $-62/4 = -15.5 \pm 1$ kcal/mol, in good agreement with other estimates (Riesner and Roemer, 1973). This value is far larger than Podder's (1972) estimate of −6.3 kcal/mol measured with oligo(G) and poly(C). The T_m of this system is below 30°, however, and residual single-strand stacking would substantially decrease the apparent ΔH. The small activation energy of 3 ± 6 kcal/mol for helix formation of transition B is consistent with the existence of an equilibrium of at least one base pair which precedes the rate determining step. Negative or zero activation energies for helix formation have been observed with a variety of other oligonucleotide systems (Riesner and Roemer, 1973).

The identity of the helix-coil transition in effect A is not completely clear, although the dependence upon concentration of its T_m and relaxation kinetics is consistent with the assignment of a bimolecular helix-coil transition (as a result of a cut in the loop of the rT-ψ arm). The lower T_m of transition A is apparently a reflection of the dependence upon concentration of its helix-coil transition relative to the monomolecular, concentration independent transition of B, and may thus be a measure of the increased stability a hairpin molecule (with a loop size 6 or larger) has over the corresponding double-stranded helix. A possible explanation for the greater ΔH of the bimolecular reaction (−78 kcal/mol) at 60° compared with the monomolecular reaction (−62 kcal/mol) at 80° would be that transition B shows incomplete "all or none" behavior, *i.e.* at its T_m transition B might have *ca.* 4.5 base pairs instead of 5.

Melting of the CCA Half. Figure 5 demonstrates that the CCA half undergoes no helix-coil transition below 60° under the conditions tested (500 mM sodium ion and 5 mM magnesium ion); the peaks at 80° in 5 mM magnesium ion and at *ca.* 95° in 500 mM sodium ion correspond to the melting of the rT-ψ helix. The flat differential melting curve below 60° in Figure 5 indicates that no additional base pairing exists in the CCA half-molecule other than in the rT-ψ arm. Thus, under the conditions we examined, the CCA half can be regarded as the rT-ψ arm with long oligonucleotide tails on the 3′ and 5′ ends.

No Double Helical Structure in the Isolated Dihydrouridine Arm. The pU half-molecule exhibited a shift in T_m of about 10° between 500 mM sodium ion and 5 mM magnesium ion, but the melting curves in both cases were broad and noncooperative. The fact that there was a continuous variation in the difference spectrum ratios throughout most of the peak indicates that it was not homogeneous under both conditions, *i.e.* two or more transitions are hidden under the peak. Temperature-jump experiments with the pU half in 500 mM sodium ion showed the complete lack of any cooperative effect which was slower than the heating rise time of the apparatus. The relaxation times as fast as the heating rise times which were seen in

these experiments are generally attributed to the melting of single-stranded, stacked conformations (Riesner and Roemer, 1973). These data constitute evidence that the separated pU half is a random coil in a solution containing 500 mM sodium ion, and that under these conditions, the dihydrouridine arm does not exist as suggested by the cloverleaf model. This conclusion may be logically extended to the 5 mM magnesium conditions, owing to the similarity in the shape of the melting profiles and in the difference spectrum ratios under both conditions. This result is not surprising, in view of the rather weak nature of the four hypothesized base pairs (two A·U, one G·U, and one G·ψ). The dihydrouridine arm of $tRNA^{Asp}$ differs considerably from that of $tRNA^{Phe}$ (yeast), which contains three G·C and one A·U base pairs and has a T_m of 70° in 0.11 M sodium ion (Roemer *et al.*, 1969).

Recombination of the Half-Molecules. Figure 6, in conjuction with Figure 5, provides evidence that there is a recombination between the pU and CCA halves in the presence of either 500 mM sodium or 5 mM magnesium ion. In the presence of magnesium a cooperative transition with difference spectrum ratios $\Delta A_{260\ nm}/\Delta A_{280\ nm}$ of 1.8 and a ΔH value of −141 kcal/mol is produced by the recombination of the two halves. The acceptor and anticodon stems must certainly be reconstituted in the mixture of the halves; both have a high G·C content (Figure 1), which should make helix formation favorable.

A simple calculation of the expected enthalpy change of the anticodon and acceptor stems at 60°, based on nearest neighbor enthalpies from the literature (Riesner and Roemer, 1973), yields −106 ± 20 kcal/mol, if the G·U base pair is evaluated as an A·U. The difference between the observed and calculated enthalpy change is beyond experimental error, and we conclude that the recombination peak represents more than helix formation in the anticodon and acceptor stems. This conclusion is corroborated by the difference spectrum ratios in the peak, which indicate that over 40% of the base pairs participating in the transition are A·U. The anticodon and acceptor stems contain just 16% A·U and 16% G·U; it may be estimated from melting curves of poly(G,A)·poly(U) that the extinction change at 260 nm melting a G·U base pair located next to an A·U base pair is roughly twice that at 280 nm (A. Lomant and J. Fresco, personal communication). The comparable ratio for A·U is much larger (Coutts, 1971). Thus, on the basis of the enthalpy change and the difference spectrum ratios we speculate that when the half-molecules recombine in the presence of magnesium, either the tertiary structure or the dihydrouridine helix or both also form. This seems reasonable since the constraints produced by the formation of the anticodon and acceptor stem helices might promote the formation of the helix in the dihydrouridine arm. Indeed, the dihydrouridine arm's helix might be a requirement for the ability to form a tertiary structure (Kim *et al.*, 1973). The ability of magnesium ion to stabilize the recombination of the two halves much more efficiently than sodium ion may be an indication of the involvement of the tertiary structure; tertiary structural transitions of tRNA have greater sensitivity to magnesium ion concentration than do normal helical transitions (Riesner and Roemer, 1973).

Finally, the ability of the aspartate tRNA synthetase to charge the half-molecules implies the existence of a tertiary structure under these conditions. The possible equilibria and conformational states of $tRNA^{Asp}$ which these data suggest are drawn diagrammatically in Figure 11. In the presence of magnesium, the intermediate states of Figure 11 are probably not occupied, since the recombination apparently proceeds in an "all or none" manner under these conditions.

The most important points to be learned from the data ob-

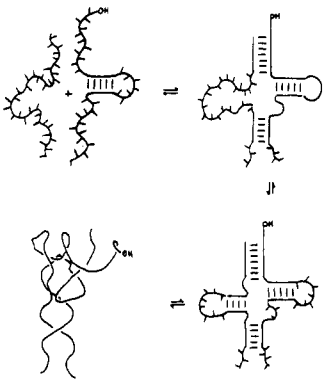

FIGURE 11: A reaction scheme showing possible equilibria involved in the recombination of the CCA and pU halves of $tRNA^{Asp}$ (yeast) in 5 mM magnesium chloride (the model for the tertiary structure of the recombined and intact $tRNA^{Asp}$ was taken from Kim *et al.*, 1973).

tained with the half-molecules are that one-half, the pU, lacks secondary structure when separated from the CCA half, and that the isolated CCA half-molecule has the very stable rT-ψ helix as its sole secondary structure. Spectroscopic, thermodynamic, and enzymatic evidence have demonstrated that the pU and CCA halves recombine to form a native, chargeable structure, in accordance with earlier work on the recombination of fragments of tRNA (Roemer *et al.*, 1969; Bayev *et al.*, 1967).

The extreme stability of the rT-ψ helix and the instability of the dihydrouridine helix permit us to understand their relative electrophoretic mobility on polyacrylamide gels (12%, pH 7): the longer half (CCA) migrates faster on the gel than the shorter half (pU) (Gangloff and Dirheimer, 1973b). This unexpected result can be explained if we assume that the CCA half has a more compact spatial configuration than the pU half.

Physical Measurements on the Intact $tRNA^{Asp}$. The time resolution of the temperature-jump method has been utilized to separate three overlapping effects in the melting curve of $tRNA^{Asp}$ (yeast) below 70° in 500 mM sodium chloride; Figure 8 shows plots of the temperature-dependent amplitudes for each effect. We have summarized the kinetic data for effects I and II of the intact $tRNA^{Asp}$ and for transition B of the isolated rT-ψ arm in Table II.

This study attempts to correlate each transition with a structural element or elements in the cloverleaf model and the three-dimensional structure of the $tRNA^{Asp}$ molecule. Of the three transitions observed with relaxation kinetics, the fastest, III, reflects the temperature perturbation of the single-strand stacking equilibrium. In addition, because of the extreme stability of the rT-ψ helix, *e.g.*, the high likelihood that all other secondary structures will melt before it, and the similarity of its melting behavior in the isolated arm and CCA half-molecules, we conclude that the rT-ψ helix has a $T_m \sim 90°$ in the intact $tRNA^{Asp}$ moleclule, and therefore need not be considered for any of the helix–coil transitions measured below 70°. Thus, there are four structural elements, the tertiary structure, and the anticodon, dihydrouridine, and acceptor stem helices, which can be assigned to the two remaining transitions (I and II) below 70°. It is worth noting that the isolated dihydrouridine helix is unstable, and that if it has any secondary structure at all in the intact $tRNA^{Asp}$, it is likely to be the most unstable of all the structural elements suggested by the cloverleaf model.

Transitions I and II lend themselves to thermodynamic interpretation, since they can be described as "all or none" reactions. The analysis of effect I must take into account several pieces of data. (a) The constant difference spectrum ratios

TABLE II: A Summary of the Relaxation Times for Effects I and II of the Intact $tRNA^{Asp}$ and for Transition B of the rT-ψ Arm.[a]

T (°C)	τ_I (msec)	τ_{II} (msec)	$\tau_{rT\text{-}\psi\ arm}$ (msec)
43.4	198 (2)		
43.6	227 (8)		
46.3	228 (2)		
46.7	277 (2)		
47.0	318 (2)		
47.1	277 (2)		
50.4	400 (2)		
51.0	476 (2)		
51.3	535 (4)		
51.4	538 (6)		
53.6	512 (3)	0.436 (3)	
54.5	457 (4)		
58.5	418 (3)	0.437 (5)	
63.6			0.0902 (2)
65.0		0.160 (3)	
66.1			0.0672 (2)
70.7			0.0693 (2)
73.0			0.0557 (2)
75.8			0.0444 (3)
79.6			0.0236 (3)
81.6			0.0201 (3)

[a] The numbers in parentheses refer to the number of observations used in calculating the relaxation time.

have a value $\Delta A_{260\ nm}/\Delta A_{280\ nm}$ of 2.7 ± 0.3. (b) The hyperchromicity at 260 nm for the transition is about 72% of the total hyperchromicity under 70° which arises from cooperative helix–coil transitions, *i.e.* the per cent hyperchromicity of effects I and II. (c) Effect I has an enthalpy change for helix formation of −101 ± 5 kcal/mol, and activation energies of −53 ± 10 and 48 ± 10 kcal/mol for helix formation and dissociation, respectively (Table I and Figure 10).

Effect II has the following characteristics: (a) constant difference spectrum ratios of 1.3; (b) 28% hyperchromicity of cooperative helix–coil transitions under 70°; (c) a ΔH for helix formation of −71 kcal/mol and activation energies of −11 and +60 kcal/mol for helix formation and dissociation, respectively (Table I and Figure 10).

A Mechanism of the Thermal Denaturation of $tRNA^{Asp}$. We wish to propose a mechanism for the melting of $tRNA^{Asp}$ in 500 mM sodium ion which is consistent with the body of data obtained with the fragments and intact tRNA. Effect I represents the strongly coupled, *e.g.* simultaneous melting of the tertiary structure, dihydrouridine helix and acceptor arm. Effect II represents the melting of the anticodon helix. Finally, effect III arises from the perturbation of the single-strand stacking equilibrium with some contribution from the rT-ψ helix at temperatures above 70°. This mechanism is pictured in Figure 12, and is justified in the following manner.

(a) DIFFERENCE SPECTRUM RATIOS. The $tRNA^{Asp}$ molecule contains just four A·U base pairs in its cloverleaf structure. Although the inclusion of G·U base pairs in a helix undergoing transition would tend to raise its values of $\Delta A_{260\ nm}/\Delta A_{280\ nm}$ (estimated value for G·U is 1.9), the difference spectrum ratios are most sensitive to the presence of A·U, which has virtually no extinction change at 280 nm while going from the helix to the coil state. Thus, it is surprising that the difference spectrum ratios of effect I indicate that the structures undergoing transition are composed of approximately 60% A·U base pairs. Obvious candidates for this transition are the only two arms which contain A·U, the dihydrouridine helix (50% A·U, *e.g.* two A·U and two G·U) and the acceptor arm (30% A·U, *e.g.* two A·U, four G·C and one G·U). Indeed, the distribution of A·U base pairs in the intact tRNA molecule is such that the surprisingly high difference spectrum ratios in I constitute a proof that the dihydrouridine helix is undergoing transition in this effect. In analogy with the tertiary structure of $tRNA^{Phe}$ (yeast), which has difference spectrum ratios of *ca.* 3.5 (Riesner and Roemer, 1973), the tertiary structure of $tRNA^{Asp}$ may also be considered as a candidate for effect I.

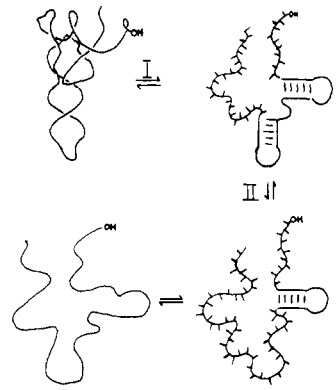

FIGURE 12: A proposed mechanism for the thermal denaturation of intact $tRNA^{Asp}$. The numerals I and II refer to effects observed with relaxation kinetics.

The difference spectrum ratios of effect II of *ca.* 1.3 correspond to 70% G·C in structure undergoing helix–coil transition. This is consistent with the assignment of the anticodon arm, which has 80% G·C.

(b) HYPERCHROMICITY. The hyperchromic contribution of the various structural elements of the cloverleaf may be calculated using the following $\Delta E_{260\ /mol}$: A·U, 4.0×10^3; G·C, 2.1×10^3 (D. Henley and J. Fresco, personal communication); and G·U, 1.6×10^3 (A. Lomant and J. Fresco, personal communication). At 260 nm, the dihydrouridine, acceptor, and anticodon helices would constitute roughly 30, 45, and 25%, respectively, of the hyperchromicity under 70°. In the first approximation, the tertiary structure can be neglected, since the tertiary structures of $tRNA^{Phe}$ (yeast), $tRNA^{Val}$ (*E. coli*), and $tRNA^{Ala}$ all show small hyperchromic changes upon melting (Riesner and Roemer, 1973). The observed 72% contribution of effect I agrees well with the sum of the dihydrouridine and acceptor helices, *e.g.* 30 + 45 = 75%, as does the hyperchromicity calculated for the anticodon helix (25%) with that observed for effect II (28%).

(c) KINETICS AND THERMODYNAMICS. The activation energy for helix formation in transition I, −53 kcal/mol, is negative and unusually large, and indicates that a preequilibrium of several base pairs is involved in helix formation, which is equivalent to saying that one or more structural elements or helices must first form before the rate determining step in the formation of ordered structure in transition I can take place. Using the nearest neighbor enthalpies of Roemer *et al.* (1969) at 50°, enthalpy changes for the dihydrouridine, acceptor, and anticodon arms are calculated to be approximately −23, −56, and −40 kcal/mol, respectively. The calculated enthalpy change for the acceptor arm equals the activation energy for helix formation in I, which includes the activation enthalpy of the rate limiting conformational element (0 − (−20) kcal/mol). Since it may be that ring closure (connecting the 5′ and 3′ ends in a

helix) takes place before the tertiary structure can form, our mechanism predicts that the acceptor arm's helix is first constituted in a preequilibrium step before the dihydrouridine helix and tertiary structure close in the rate determining step.

The enthalpy change of −101 kcal/mol for the helix to coil transition I indicates that two or more structural (cloverleaf) elements are involved in the transition. According to our mechanism, the ΔH for transition I represents the sum of the enthalpy changes for the melting of the dihydrouridine and acceptor helices plus the tertiary structure, *e.g.* $\Delta H_I = -79 + \Delta H_{ter\ strc}$ kcal/mol. The enthalpy change for the melting of the tertiary structure of $tRNA^{Asp}$ cannot be calculated; literature values for other tRNA molecules range from −33 to −45 kcal/mol (Riesner and Roemer, 1973). Thus, by difference, the ΔH value we obtain for the tertiary structure is −22 kcal/mol, which seems reasonable when compared to the values above.

It is interesting to compare effect I, in 500 mM sodium ion, with the recombination peak measured for the two half-molecules in 5 mM magnesium ion. According to our analysis both peaks have the same structural elements (dihydrouridine and acceptor arms, tertiary structure) undergoing transition, with the recombination peak containing the anticodon helix in addition. The difference in enthalpy changes between the two transitions, whose T_m values differ by 10°, is 40 kcal/mol, which agrees well with the calculated value for the anticodon helix at 60°, −43 kcal/mol.

The enthalpy change for effect II is higher than that calculated for the anticodon helix, *i.e.* −71 kcal/mol observed *vs.* −43 kcal/mol calculated. This difference in ΔH can be in part attributed to the difficulty in making the temperature-jump measurements and consequently in the high error associated with the values, and in part to the lack of quantitative data for G·U base pairs. Differences of this magnitude between calculated and observed enthalpy values for some tRNA transitions have been observed before (Riesner and Roemer, 1973). The activation energies of −11 and +60 kcal/mol for helix recombination and dissociation of effect II, respectively, are typical for short single helices (Riesner and Roemer, 1973).

The predicted T_m for the anticodon helix in 1 M sodium ion, according to Gralla and Crothers (1973), is 87°. Assuming a value of *ca.* 20° for $dT_m/d \log [Na^+]$ for the helix, this would be 80° in 0.5 M sodium ion. The observed value of 61° for effect II is much lower; this may be due to some electrostatic destabilization from the intact neighboring rT-ψ arm, and to the inaccuracy of the quantitative data on interior G·U base pairs.

Obviously, the thermodynamic data cannot be treated in an exact, quantitative manner. However, the spectral and thermodynamic data observed with both the fragments and intact molecule of $tRNA^{Asp}$ support the simultaneous opening of the tertiary structure, dihydrouridine, and accepter helices in the first melting step of the intact molecule, followed by the anticodon helix and finally by the thermal denaturation of the rT-ψ arm.

Does $tRNA^{Asp}$ Have the Same Conformation as 0.5 M Sodium and 5 mM Magnesium Ions? Although a definitive answer cannot be given to this question because the enzymatic assay of $tRNA^{Asp}$ cannot be carried out at high ionic strength, a number of studies on simple polynucleotides and oligonucleotides have shown that the electrostatic effect of magnesium ion can be mimicked by higher concentrations of sodium ion (Riesner and Roemer, 1973). The special case of tertiary structure is more difficult to analyze, since it is known to be very sensitive to the presence of divalent cations. Phase diagrams of $tRNA^{fMet}$ (*E. coli*) proposed by Cole *et al.* (1972) show no special magnesium region; the tertiary structure of $tRNA^{Phe}$ (yeast), however, has an absolute requirement for divalent cation (D. Riesner, personal communication). The spectral and thermodynamic data above imply that the tertiary structure of $tRNA^{Asp}$ (yeast) is present in 0.5 M sodium ion, although more evidence would be needed to provide unambiguous proof.

How Does $tRNA^{Asp}$ (Yeast) Differ from Other tRNA Molecules? The unusual feature of our model for the thermal denaturation of $tRNA^{Asp}$ is the stabilization of the dihydrouridine helix far above its T_m in 500 mM sodium ion by the intact molecule. The mechanism implies that the tertiary structure is responsible for this stabilization. The instability of the dihydrouridine helix has been noted for two other tRNA species. Oligonucleotide binding experiments (Uhlenbeck *et al.*, 1972) and high-resolution nuclear magnetic resonance (nmr) measurements (Wong *et al.*, 1973) on the native and denatured forms of $tRNA_3^{Leu}$ (yeast) have demonstrated that the dihydrouridine helix melts as the native conformer is converted (by removing magnesium or lowering the ionic strength) to the denatured, *i.e.* as the native tertiary structure melts, so does the dihydrouridine helix. Cole and Crothers (1972) have also hypothesized that the cloverleaf form of $tRNA^{fMet}$ (*E. coli*) which is obtained from an early melting transition in 0.17 M sodium ion may lack its dihydrouridine helix. On the basis of melting curves and temperature-jump experiments, these authors concluded that the tertiary structure and dihydrouridine helix could melt simultaneously but independently. Although some tRNA species such as $tRNA^{Phe}$ (yeast) have a rather stable dihydrouridine helix (Riesner *et al.*, 1973), the helix is the shortest of the main arms of the cloverleaf model and its relative instability may be a general feature of most tRNAs.

Acknowledgments

The authors wish to thank Professor G. Maass and Drs. Detlev Riesner and Roland Roemer for many informative discussions and suggestions, and Renate Hach, Gisela Fay, and Wolfgang Haupt for their fine technical assistance. They are also indebted to Dr. Frens Peters for the use of his computer programs in the analysis of the kinetic data.

Appendix

The determination of the reaction and activation enthalpies of a bimolecular reaction when the concentration of the reactants in unknown but equal is shown. Let the equilibrium of a helix, H, with two randomly coiled oligonucleotides, C_1 and C_2, be represented by

$$C_1 + C_2 \underset{k_D}{\overset{k_R}{\rightleftharpoons}} H \qquad (I)$$

where k_R and k_D are the recombination and dissociation rate constants, respectively. The association constant K is

$$K = [H]/[C_1][C_2] = k_R/k_D \qquad (II)$$

At low temperatures, the equilibrium is completely on the side of the helix form, which has a concentration of $[H]_0$, which is also the total concentration of C_1 and C_2. As the temperature is raised, a portion of the helix melts which is equal to the concentration of either C_1 or C_2. Thus, the extent of reaction, θ, may be defined as

$$\theta = [C_2]/[H]_0 \qquad (III)$$

Then

$$K = ([H]_0 - [C_2])/[C_2]^2 = (1 - \theta)/\theta^2[H]_0 \qquad (IV)$$

Thus

$$K[H]_0 = (1 - \theta)/\theta^2 = [H]_0 k_R/k_D \qquad (V)$$

The quantity θ and therefore $K[H]_0$ are experimentally accessible from the differentiated melting curve by integration. Plotting ln $(K[H]_0)$ against $1/T$ yields a straight line with a slope of $-\Delta H/R$, *i.e.*

$$\ln (K[H]_0) = -\Delta H/RT + \Delta S/R + \ln [H]_0 \quad \text{(VI)}$$

It can be shown (Roemer *et al.*, 1969) that the relaxation rate constant for a bimolecular process involving equal concentrations of reactants is equal to

$$1/\tau = (4k_R k_D[H]_0 + k_D^2)^{1/2} \quad \text{(VII)}$$

Substituting V into VII yields

$$1/\tau^2 = 4k_R^2[H]_0/K + k_R^2/K^2 \quad \text{(VIII)}$$

Rearranging

$$1/k_R^2 = \tau^2(4[H]_0/K + 1/K^2) \quad \text{(IX)}$$

Multiplying each side by $1/[H]_0^2$ gives

$$1/(k_R[H]_0)^2 = \tau^2(4/K[H]_0 + 1/(K[H]_0)^2) \quad \text{(X)}$$

The values for $K[H]_0$ can be obtained according to eq V. Substitution and rearrangement yields

$$k_R[H]_0 = \left(\frac{1-\theta}{\theta^2}\right)\frac{1}{\tau}\left[1\Big/\sqrt{4\left(\frac{1-\theta}{\theta^2}\right)+1}\right] \quad \text{(XI)}$$

The two variables on the right-hand side of eq XI are experimentally accessible. For a given temperature T, θ can be calculated from the melting curve and τ is obtained from the temperature-jump experiment. Similar to eq 6, a plot of ln $(k_R[H]_0)$ against $1/T$ will yield a straight line with a slope of $-\Delta E_R/R$

$$\ln (k_R[H]_0) = \frac{-\Delta E_R}{RT} + \frac{\Delta S^*}{R} + \ln [H]_0 \quad \text{(XII)}$$

where ΔE_R is the activation enthalpy for the recombination reaction. Using II and III, an expression for k_D may be derived.

$$k_D = \frac{k_R[H]_0}{(1-\theta)/\theta^2} \quad \text{(XIII)}$$

References

Adams, A., Lindahl, T., and Fresco, J. R. (1967), *Proc. Nat. Acad. Sci. U. S. 57*, 1684.

Bayev, A. A., Fodov, I., Mirzabekov, A. D., Axelrod, V. D., and Kazarinova, L. Y. (1967), *Mol. Biol. 1*, 859.

Blake, R. D., Fresco, J. R., and Langridge, R. (1970), *Nature (London) 225*, 32.

Brown, R. S., Clark, B. F. C., Coulson, R. R., Finch, J. T., Klug, A., and Rhodes, D. (1972), *Eur. J. Biochem. 31*, , 130.

Cole, P. E., and Crothers, D. M. (1972), *Biochemistry 11*, 4368.

Cole, P. E., Yang, S. K., and Crothers, D. M. (1972), *Biochemistry 11*, 4358.

Coutts, S. M. (1971), *Biochim. Biophys. Acta 232*, 94.

Cox, R. A. (1970), *Biochem. J. 120*, 539.

Cramer, F., von der Haar, F., Holmes, K. C., Saenger, W., Schlimme, E., and Schultz, G. E. (1970), *J. Mol. Biol. 51*, 523.

Fresco, J. R., Adams, A., Ascione, R., Henley, D. D., and Lindahl, T. (1966), *Cold Spring Harbor Symp. Quant. Biol. 31*, 527.

Gangloff, J., and Dirheimer, G. (1973a), *Biochim. Biophys. Acta 294*, 263.

Gangloff, J., and Dirheimer, G. (1973b), *Biochemie*, submitted for publication.

Gangloff, J., Keith, G., Ebel, J. P., and Dirheimer, G. (1971), *Nature(London), New Biol. 230*, 125.

Gangloff, J., Keith, G., Ebel, J. P., and Dirheimer, G. (1972a), *Biochim. Biophys. Acta 259*, 198.

Gangloff, J., Keith, G., Ebel, J. P., and Dirheimer, G. (1972b), *Biochim. Biophys. Acta 259*, 210.

Gralla, J., and Crothers, D. M. (1973), *J. Mol. Biol. 73*, 497.

Kearns, D. R., Patel, D., Schulman, R. G., and Yamane, T. (1971), *J. Mol. Biol. 61*, 265.

Keith, G., Gangloff, J., and Dirheimer, G. (1971), *Biochimie 53*, 123.

Kim, S. H., Quigley, G., Suddath, F. L., McPherson, A., Sneden, D., Kim, J. J., Weinzierl, J., and Rich, A. (1973), *Science 179*, 285.

Mans, R. J., and Novelli, G. D. (1961), *Arch. Biochem. Biophys. 94*, 48.

Podder, S. K. (1972), *Biopolymers 11*, 1395.

Riesner, D., Maass, G., Thiebe, R., Philippsen, P., and Zachau, H. G. (1973), *Eur. J. Biochem. 36*, 76.

Riesner, D., and Roemer, R. (1973), *in* Physico-Chemical Properties of Nucleic Acids, Duchesne, J., Ed., New York, N. Y., Academic Press, p 237.

Riesner, D., Roemer, R., and Maass, G. (1970), *Eur. J. Biochem. 15*, 85.

Roemer, R., Riesner, D., Coutts, S. M., and Maass, G. (1970a), *Eur. J. Biochem. 15*, 77.

Roemer, R., Riesner, D., and Maass, G. (1970b), *FEBS (Fed. Eur. Biochem. Soc.) Lett. 10*, 352.

Roemer, R., Riesner, D., Maass, G., Wintermeyer, W., Thiebe, R., and Zachau, H. G. (1969), *FEBS (Fed. Eur. Biochem. Soc.) Lett. 5*, 15.

Scheffler, I. E., Elson, E. L., and Baldwin, R. L. (1968), *J. Mol. Biol. 36*, 291.

Schmidt, J., Buchardt, B., and Reid, B. R. (1970), *J. Biol. Chem. 245*, 5743.

Uhlenbeck, O. C., Borer, P. N., Dengler, B., and Tinoco, I., Jr. (1973), *J. Mol. Biol. 73*, 483.

Uhlenbeck, O. C., Chirikjian, J., and Fresco, J. R. (1972), *Fed. Proc., Fed. Amer. Soc. Exp. Biol. 31*, 422.

Wintermeyer, W., Thiebe, R., Zachau, H. G., Riesner, D., Roemer, R., and Maass, G. (1969), *FEBS (Fed. Eur. Biochem. Soc.) Lett. 5*, 23.

Wong, Y. P., Kearns, D. R., Schulman, R. G., Yamane, T., Chang, S., Chirikjian, J. G., and Fresco, J. R. (1973), *J. Mol. Biol. 74*, 403.

Zachau, H. G. (1969), *Angew. Chem. 81*, 717.